Coupling of Protein Surface Hydrophobicity Change to ATP Hydrolysis by Myosin Motor Domain

Makoto Suzuki*, Junji Shigematsu,# Yoshifumi Fukunishi,§ Yoshie Harada,¶ Toshio Yanagida,¶‖ and Takao Kodama#

*Department of Metallurgy, Faculty of Engineering, Tohoku University, Sendai 980-77 Japan, National Institute for Advanced Interdisciplinary Research/Mechanical Engineering Laboratory, AIST, Tsukuba 305, Japan; #Laboratory of Molecular Enzymology, Kyushu Institute of Technology, Iizuka 820, Japan; §Department of Chemistry, Rutgers, The State University of New Jersey, New Brunswick, New Jersey 08855-0939 USA; ¶Yanagida Biomotron Project, ERATO, JRDC, Minoh 562, Japan; and ‖Department of Biophysical Engineering, Faculty of Engineering Science, Osaka University, Toyonaka 560, Japan

ABSTRACT Dielectric spectroscopy with microwaves in the frequency range between 0.2 and 20 GHz was used to study the hydration of myosin subfragment 1 (S1). The data were analyzed by a method recently devised, which can resolve the total amount of water restrained by proteins into two components, one with a rotational relaxation frequency (f_c) in the gigahertz region (weakly restrained water) and the other with lower f_c (strongly restrained water). The weight ratio of total restrained water to S1 protein thus obtained (0.35), equivalent to 2100 water molecules per S1 molecule, is not much different from the values (0.3–0.4) for other proteins. The weakly restrained component accounts for about two-thirds of the total restrained water, which is in accord with the number of water molecules estimated from the solvent-accessible surface area of alkyl groups on the surface of the atomic model of S1. The number of strongly restrained water molecules coincides with the number of solvent-accessible charged or polar atoms. The dynamic behavior of the S1-restrained water during the ATP hydrolysis was also examined in a time-resolved mode. The result indicates that when S1 changes from the S1·ADP state into the S1·ADP·P_i state (ADP release followed by ATP binding and cleavage), about 9% of the weakly restrained waters are released, which are restrained again on slow P_i release. By contrast, there is no net mobilization of strongly restrained component. The observed changes in S1 hydration are quantitatively consistent with the accompanying large entropy and heat capacity changes estimated by calorimetry (Kodama, 1985), indicating that the protein surface hydrophobicity change plays a crucial role in the enthalpy-entropy compensation effects observed in the steps of S1 ATP hydrolysis.

INTRODUCTION

The hydration of proteins is of fundamental importance to our understanding of their folding and functions (Eisenberg and McLachlan, 1986; Tanford, 1980). Of various methods used to study protein hydration (for a recent review, see Gregory, 1995), dielectric spectroscopy is a unique technique (Grant et al., 1978; Pethig, 1979; Takashima, 1989) that yields direct information on the rotational mobility of water hydrating proteins and the volume of hydration shells. However, the technique has not been used in a time-resolved mode to investigate the dynamic behavior of water hydrating proteins during enzyme catalysis.

Recently we developed a method (Suzuki et al., 1996) of microwave dielectric spectroscopy to measure the total number (N_t) of restrained waters on protein and to resolve N_t into N_w (the number of "weakly restrained" waters with a rotational relaxation frequency, f_c, in the gigahertz region) and N_s (the number of "strongly restrained" waters, with lower f_c). This method has a time resolution of 5 s, which is applicable to ATP hydrolysis by the myosin motor domain (S1). The protein is available in quantity and is one of the best characterized in terms of kinetics (Woledge et al., 1985), energetics (Kodama, 1985), and three-dimensional atomic structure (Rayment et al., 1993).

In the present work we have attempted to estimate N_w and N_s for S1 and have obtained values that are in good agreement with those theoretically calculated from its 3D structure. In addition, a small but significant fraction of the weakly restrained waters are mobilized without net mobilization of the strongly restrained water during the ATPase cycle. Implication of these results is discussed on the basis of calorimetric data for S1 ATP hydrolysis.

MATERIALS AND METHODS

S1 was prepared from rabbit skeletal muscle myosin by chymotryptic digestion (Weeds and Taylor, 1975), concentrated by ammonium sulfate to a protein concentration of 20–40 mg/ml, and dialyzed against buffer A containing 20 mM KCl, 5 mM $MgCl_2$, and 10 mM 3-(*N*-morpholino)propanesulfonic acid (pH 7.0). Protein concentration was determined using the absorbance coefficient at 280 nm to be 0.75 cm^{-1} for 1 mg/ml. ATP hydrolysis was measured by the malachite green method (Kodama et al., 1986).

Measurements

The dielectric spectra were obtained in a microwave network analyzer (Hewlett Packard 8720C) with an open-end flat-surface coaxial probe fixed in a glass cell, which was kept at 20.0 ± 0.01°C by a circulating thermobath. The cell was filled with dialyzed S1 solution degassed under a reduced pressure, into which microwaves in the frequency range between

Received for publication 13 June 1996 and in final form 15 October 1996.

Address reprint requests to Dr. Makoto Suzuki, Department of Metallurgy, Tohoku University, Aramaki-aza-Aoba, Sendai 980-77, Japan. Tel.: 81-22-217-7303; Fax: 81-22-217-7374; E-mail: msuzuki@material.tohoku.ac.jp.

0006-3495/97/01/18/06 $2.00

0.2 and 20 GHz were introduced through the probe. For each measurement dielectric spectra were obtained every 4.4 s and averaged.

Analysis

Fig. 1 shows the dielectric properties of S1 solution and hydrated S1. ϵ_a^* and ϵ_{ap}^* are the complex dielectric constants of buffer solution and S1 solution, respectively. The rapid decrease in ϵ_a^* and ϵ_{ap}^* at low frequencies of 0.2–1.5 GHz corresponds to the ionic conduction. The region of 1.5–20 GHz corresponds to the orientational relaxation of water, including free water and restrained water on protein. For the hydrated solute, the complex dielectric constant ϵ_q^* (*triangles*) is related to its volume fraction ϕ by the equation proposed by Hanai (1960),

$$\frac{\varepsilon_{ap}^* - \varepsilon_q^*}{\varepsilon_a^* - \varepsilon_q^*}\left(\frac{\varepsilon_a^*}{\varepsilon_{ap}^*}\right)^{1/3} = 1 - \phi.$$

The value ϕ and the relaxation frequency f_c of hydrated solute were estimated by combined use of this equation with the Wagner equation (1914) and the Debye fitting procedure (Suzuki et al., 1996), for which an outline is given here.

The basic assumption is that a hydrated protein is a shelled sphere. The dielectric constant of such a sphere at the high frequency limit ($\epsilon_{q\infty}$, ϵ_q^* for $f \to \infty$) is given by the Wagner equation with the dielectric constant of core protein (ϵ_p), its volume, the dielectric constant of hydration shell (ϵ_h), and ϕ. We set $\epsilon_p = 2.5$ and $\epsilon_h = 5.6$. Assuming an initial value for ϕ, ϵ_q^* is calculated by the Hanai equation as described above, which is then fitted over a frequency range from 2.5 to 8 GHz by a single Debye relaxation function,

$$\varepsilon_q^* \approx \varepsilon_{q\infty} + (\varepsilon_{qs} - \varepsilon_{q\infty})/(1 + jf/f_c).$$

Extrapolating to the high frequency limit ($f \to \infty$), this equation gives an estimate of $\epsilon_{q\infty}$. The value thus obtained is not generally equal to the $\epsilon_{q\infty}$ value given by the Wagner equation, so that the whole calculation is iterated by changing the ϕ value until they coincide with each other, which then gives best estimates for ϕ and f_c.

RESULTS

Hydration of S1

Fig. 2 shows the dielectric excluded volume fractions of bare protein (v), protein with a full hydration shell (ϕ), and with a strongly restrained hydration shell (ϕ_1) in solution. v

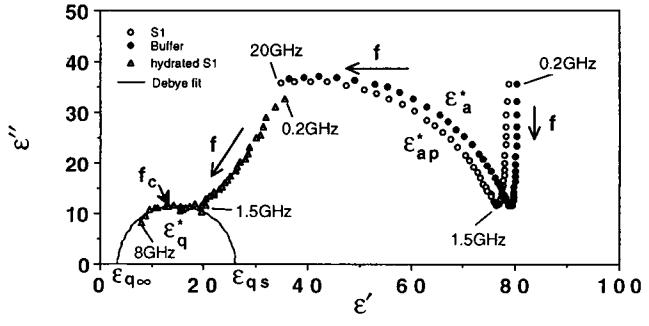

FIGURE 1 The Cole-Cole plots showing the dielectric properties of S1 solution and hydrated S1. The complex dielectric constant $\epsilon^* = \epsilon' - j\epsilon''$ is displayed as a function of frequency (f): $\epsilon_a^* = \epsilon_a' - j\epsilon_a''$ for buffer (●), $\epsilon_{ap}^* = \epsilon_{ap}' - j\epsilon_{ap}$ for S1 solution (○), and $\epsilon_q^* = \epsilon_q' - j\epsilon_q''$ for hydrated protein (△), calculated with the equation in the text.

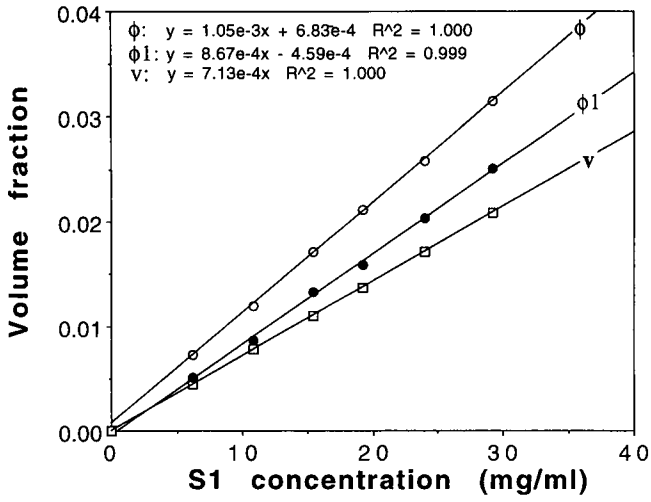

FIGURE 2 The volume fractions of bare protein (v) and protein with a strongly restrained hydration shell (ϕ_1) and with a full hydration shell (ϕ).

is given by

$$v = cM_w s_v/1000,$$

where c, s_v, and M_w are the protein concentration in mol/liter, the partial specific volume (0.713 liter/kg) (Tamura et al., 1993), and the molecular weight (110,000) of protein S1, respectively. ϕ was calculated from the high frequency limit of the dielectric spectrum of hydrated solute ϵ_q^* as described in Materials and Methods. The total number of restrained waters (N_t) is given by

$$N_t = 55.6(\phi - v)\rho_0/c,$$

where ρ_0 is the density of solvent in kg/liter. ϕ_1 was calculated from the low-frequency limit of the fitting curve of a single Debye relaxation function to the dielectric spectrum of S1 solution ϵ_{ap}^*, according to the method of Wei et al. (1994). The number of strongly restrained waters (N_s) with a relaxation frequency much lower than 1 GHz is given by

$$N_s = 55.6(\phi_1 - v)\rho_0/c.$$

Hence the number of weakly restrained waters is given by

$$N_w = N_t - N_s.$$

The results of these calculations are summarized in Table 1. The weight of total restrained waters per protein weight for S1 (0.35) is not much different from the corresponding values (0.34–0.42) for five other proteins (cytochrome c, myoglobin, ovalbumin, bovine serum albumin, and hemoglobin) examined in our previous study. However, the N_w/N_t value for S1 (0.67) is larger than the values for other proteins (0.26–0.58), which indicates that the S1 molecular surface is rather hydrophobic in nature (see Discussion).

TABLE 1 Hydration and its change of S1 during the ATPase cycle and related calorimetric data

	Observed	Calculated
Number of restrained waters*		
Total restrained water (N_t)	2130 ± 60	2000
Strongly restrained water (N_S)	720 ± 50	600
Weakly restrained water (N_W)	1410 ± 80	1400
Nucleotide-induced hydration change#		
ΔN_t for (S1 · ADP → S1 · ADP · P_i)	−122 ± 18	−100 to −160
ΔN_S for (S1 · ADP → S1 · ADP · P_i)	−2 ± 2	—
ΔN_t for (S1 → S1 · ADP)	+17 ± 13	—
ΔN_S for (S1 → S1 · ADP)	−6 ± 13	—

Thermodynamic parameters§

	ΔH_u (kJ/mol)	ΔS_u (J/K mol)	ΔC_{Pu} (J/K mol)
S1 · ADP + ATP →			
S1 · ADP · P_i + ADP	+32	+240	−2800
S1 · ADP · P_i → S1 · ADP + P_i	−52	−230	+2600
ATP → ADP + P_i	−20	+10	−200
$-CH_2-$ (nonpolar) →			
$-CH_2-$ (aqueous)	<4	−5 to −7	+50 to +80

*Observed values are the means (± SEM) of 13 measurements with seven different S1 preparations similar to those described and analyzed as in Fig. 1. Calculated values are those for the S1 molecular structure. N_W is equal to the total SAS of surface-exposed apolar moieties divided by the average water occupancy of 9 Å^2 over the S1 surface. N_S was calculated as the total number of surface-exposed O, N, and S that act as a hydrogen acceptor or donor with the SAS > 8Å^2, excluding -CONH- (Rossky and Karplus, 1979).

#Observed values are the means (± SEM) of data from six independent experiments (as in Fig. 3 *A*), which were corrected for the magnitude of the initial phosphate burst (~0.63). The calculated value was estimated using the calorimetric data at the bottom of the table, assuming that ΔS_u and ΔC_{Pu} for the transition (S1 · ADP → S1 · ADP · P_i) are solely ascribed to the transfer of $-CH_2-$ from hydrophilic to hydrophobic environments, which is justified by a good agreement between the ratio of ΔS_u(S1 · ADP · P_i → S1 · ADP)/ΔS_u for the $-CH_2-$ transfer (230/6 = 38) and the corresponding ratio of ΔC_{Pu} (2600/65 = 40). Assuming that on average three water molecules are restrained by each $-CH_2-$ (Goldammer and Hertz, 1970), the number of water molecules would then be 40 × 3 = 120.

§Data in unitary quantities from Kodama (1985), except for solvation data of $-CH_2-$ calculated from Tanford (1980).

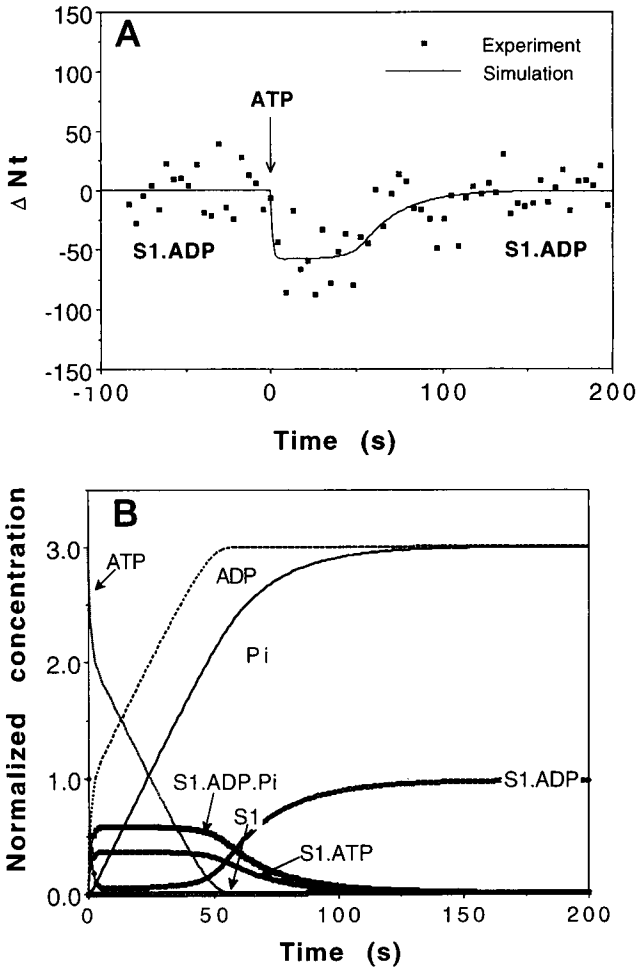

FIGURE 3 ATP-induced change of number of total water molecules restrained around S1. (*A*) A typical time course of N_t before and after the addition of a threefold molar excess of ATP to S1 with bound ADP preformed from stoichiometric ATP. The value ΔN_t for the transition from the S1·ADP state to the S1·ADP·P_i-rich state was calculated by subtracting the *N* value averaged over a period between −25 and 0 s or between 110 and 200 s from that between 0 and 25 s. For this specific case, the value was −58 ± 25. (*B*) Simulation of S1-ATPase reaction: [S1] = [MgADP] = 0.3 mM and [MgATP] = 0.9 mM. Taking into account the initial phosphate burst (0.63) and the steady-state rate of ATP hydrolysis (0.053 s^{-1}) at 20.0°C, the rate constants were adopted from Woledge et al. (1985) for the following steps: 1 (S1 + ATP ⇄ S1·ATP), $k_1 = 10^6$ s^{-1} M^{-1}, $k_{-1} = 0$; 2 (S1·ATP ⇄ S1·ADP·P_i), $k_2 = 100$ s^{-1}, $k_{-2} = 62$ s^{-1}; 3 (S1·ADP·P_i ⇄ S1·ADP + P_i), $k_3 = 0.075$ s^{-1}, $k_{-3} = 0.75$ s^{-1} M^{-1}; 4 (S1·ADP ⇄ S1 + ADP), $k_4 = 1$ s^{-1} and $k_{-4} = 2 \times 10^5$ s^{-1} M^{-1}.

Hydration change coupled to ATPase cycle

We then examined the hydration change during the ATPase cycle. Fig. 3 *A* shows a typical time course of ΔN_t after the addition of a threefold molar excess of MgATP to S1 with bound ADP. At $t = 0$, a 0.2-ml portion of 100 mM MgATP adjusted to pH 7.0 in buffer A was injected into 20 ml of S1 solution (36.2 mg/ml) that had been preincubated with 0.33 mM MgATP. Mixing was completed within 5 s, and the temperature change caused by injection was negligible (<0.02°C). The dielectric spectrum was obtained every 4.4 s. Because a small offset of the spectra was caused by the addition of ATP, a correction was made by evaluating its magnitude on the addition of 1 mM MgADP to S1 saturated with ADP in buffer A in separate experiments. When added to buffer A not containing S1, MgATP and MgADP caused the spectral offsets in the same direction with almost the same magnitude, so that use of ADP for offset correction was justifiable. On the other hand, no correction was made for the effect of ATP hydrolysis, because it should be negligibly small, as expected from the effects of MgATP and MgADP as just described and because 1 mM P_i did not affect the dielectric spectrum in the gigahertz region required for the analysis of ATP-induced hydration changes in S1.

As shown in Fig. 1, the spectrum of ϵ_q^* is approximated with a Debye half-circle, showing a f_c around 4 GHz. Therefore the change of ϵ_q' for $f > 2.5$ GHz is proportional to the change of $\delta = \epsilon_{qs} - \epsilon_{q\infty}$, then to the volume of the hydration shell. We hence monitored ϵ_q' values at five different frequency points (2.52, 3.17, 3.99, 5.02, and 6.32 GHz) and averaged them to estimate the weakly restrained hydration volume. The calibration was made at a few time points immediately after the addition of ATP ($0 \text{ s} < t < 25 \text{ s}$) and after the exhaustion of ATP ($110 \text{ s} < t < 200 \text{ s}$) by calculating N_t and N_s as described above.

At $t = 0$, N_t (*squares*) rapidly decreased to a steady level, which then slowly returned to the level before the addition of ATP. The reaction sequence is that the ADP initially bound to S1 is displaced by ATP, followed by its cleavage to form an equilibrium mixture of intermediates with bound ATP and with bound ADP + P_i. These processes are fast, but the following P_i release is so slow that the mixture is the major intermediate with an excess of ATP.

Thus during the ATPase cycle S1 undergoes a cyclic change between hydration and dehydration, with mobilization of approximately 6% of the total S1-hydrating water (Table 1). These mobile waters are mostly weakly restrained, because the single Debye-type half-circle fitted to the Cole-Cole plots of ϵ_q^* gave $f_c = 4 \pm 1$ GHz. In fact, the corresponding value of ΔN_s was negligibly small. There was no significant difference in either N_t or N_s between the S1 with and without bound ADP.

DISCUSSION

Weakly restrained water

NMR studies showed that a few water molecules are restrained by each apolar moiety (for example a -CH_2- group) of hydrophobic solutes (Goldammer and Hertz, 1970). Using a two-component solute emulsion analysis by the Hanai equation, we have studied the hydration shells around the apolar moieties of a series of hydrophobic α-amino acids (Suzuki et al., manuscript submitted for publication). The relaxation frequencies of hydrated alkyl side chains around 4.5 GHz are clearly separated from the orientational relaxation frequency of amino acid dipoles. This result is in good agreement with a molecular dynamics calculation that the hydration shell around apolar moieties has a three-times longer rotational correlation time than bulk water (Rossky and Karplus, 1979). Our result also shows that on average three water molecules are restrained by each -CH_2- group. Therefore, we can attribute the weakly restrained water with f_c around 4.5 GHz to hydrophobic hydration. By contrast, water is restrained strongly in the close vicinity of surface-exposed charged or polar atoms.

A hydration model of S1

By using the SegMod program (Levitt, 1992), a molecular model of S1 with amino acid side chains can now be reconstructed (Ruppel and Spudich, 1996) from the PDB

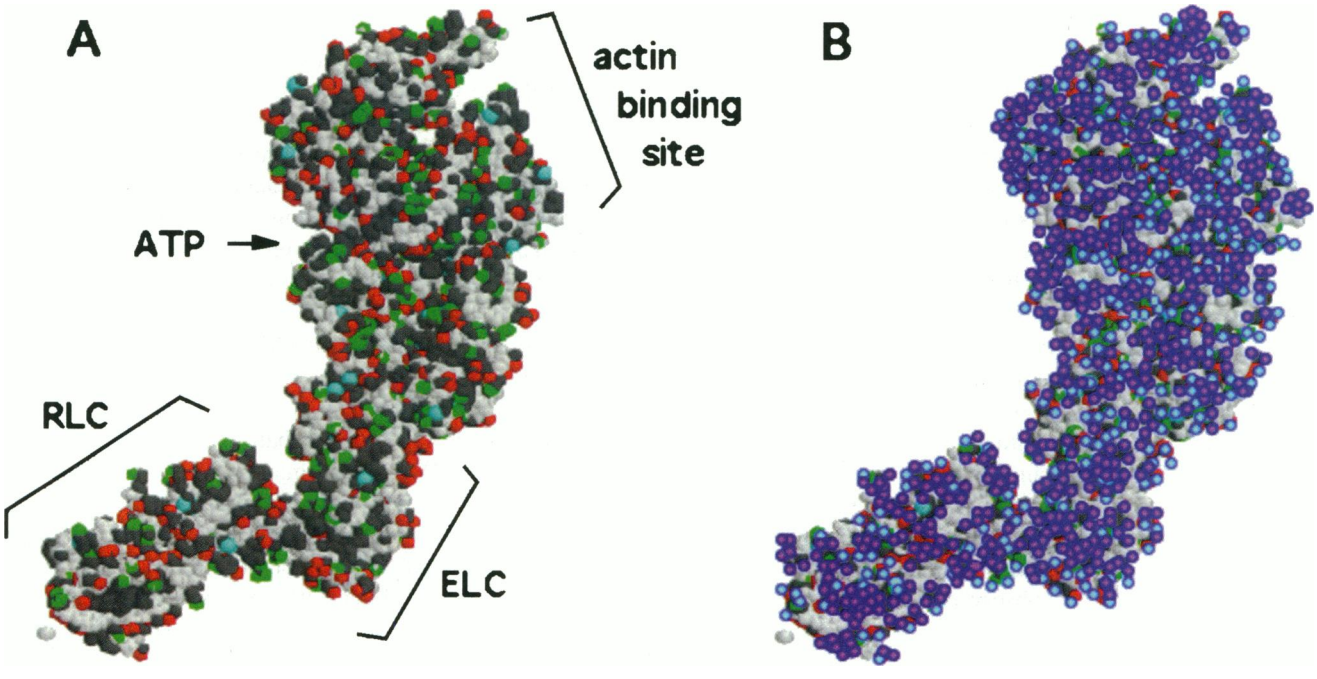

FIGURE 4 (*A*) Myosin subfragment-1 reconstructed by SegMod (Ruppel and Spudich, 1996). Red, oxygen; green, nitrogen; cyan, sulfur; gray, carbon of side chain; white, skeleton atoms including nitrogen and oxygen. Note that our chymotriptic S1 does not have the RLC domain. The image was created using RasMol version 2.6. (*B*) Theoretical image of hydration state of S1. Each blue circle indicates a water molecule placed on a surface-exposed polar atom. Magenta circles indicate water molecules covering surface-exposed hydrocarbons.

α-carbon data (Rayment et al., 1993), as shown in Fig. 4 *A*. Although it is not necessarily unique (because some errors, if not large, could have been brought into the calculation), it is tempting to estimate the number of water molecules restrained on the surface of this model.

Taking into account that the chymotryptic S1 lacks the regulatory light chain (RLC), we first calculated the total solvent-accessible surface (SAS) area for hydrophobic carbons (not bonded to O, N, or S) on the surface of S1. Division of the total SAS area by the occupation area of a water molecule (9 $Å^2$ calculated from the radius of 1.4 Å and spacing) gives an estimate of the number of water molecules restrained around apolar moieties. We also counted the number of surface-exposed charged or polar atoms with SAS > 8 $Å^2$. An assumption was made in both calculations that the missing residues in the PDB data (1–3, 205–215, 572–574, 627–646, 732–737, ELC1-4, and ELC52-62) are fully exposed to the solvent. The N values calculated from these estimates are shown in Table 1, with which the observed values show an excellent agreement. Our snapshot image of hydrated S1 is shown in Fig. 4 *B*, where a water molecule is placed on each surface-exposed polar or charged atom (*blue circle*), and surface-exposed apolar moieties are covered according to the calculation described above (*magenta circle*).

ATP-induced changes in S1 surface hydrophobicity

The sign and large magnitude of ΔS and ΔC_p for ATP cleavage and subsequent P_i release in the S1 ATP hydrolysis cycle observed by calorimetry are characteristic of changes in hydrophobic hydration (Kodama, 1985). By contrast, the values of ΔS and ΔC_p for ADP release are small and almost cancel out those for ATP binding. Thus ADP release and ATP binding followed by its cleavage can be lumped together for thermodynamic consideration of the rapid phase in the ATPase cycle. We can then calculate the number of mobile water molecules during the rapid and slow phases corresponding to the reaction sequence in our measurement of hydration change coupled to the ATPase cycle. For this purpose we calculated the thermodynamic values for alkyl group transfer from apolar solvent into water from the data given by Tanford (1980), as shown in Table 1. It should be pointed out that the ΔH increment in such transfers is negligibly small with an increase in alkyl chain length of alcohols and alkanes, indicating that the hydrophobic interaction, accompanied by large ΔC_p values, is overwhelmingly entropic in nature. The value for the number of mobile water molecules thus obtained is again in good agreement with the observed values (Table 1). It is roughly equivalent to an involvement of 40 or more methylene ($-CH_2-$) moieties. Although its exact structural basis remains to be elucidated, it is evident that these moieties are segregated from the bulk water by being buried in the interior of the protein and/or associating with themselves side by side when S1 is in the S1·ADP·P_i state.

Although there have been a few examples of mobilization of protein-restrained water or changes in protein hydration in enzyme catalysis suggested by indirect methods (Rand et al., 1993, and related references therein), the present result is the first to provide direct evidence for hydration and dehydration in a particular step or steps lumped together in the catalytic cycle of an enzyme.

Gopal and Burke (1996) recently observed that in phenyl hydrophobic chromatography, S1 is eluted significantly faster in the presence of ATP than in the presence of ADP or under nucleotide-free conditions, suggesting an ATP-induced decrease in S1 hydrophobicity. Our result is compatible with this observation. On the other hand, studying the effects of osmotic stress with polyethylene glycol on the kinetics of ATP hydrolysis by S1, Highsmith et al. (1996) suggested that none of the steps in S1 ATP hydrolysis cycle are accompanied by substantial hydration changes. However, the osmotic stress ($0.5–5 \times 10^6$ dyne/cm^2) used without causing protein precipitation in their study seems to be too small to affect the kinetics, because a much higher stress (up to 2.5×10^7 dyne/cm^2) was successfully used to detect hydration changes involving a small number of water molecules (<100) in the catalytic cycle of hexokinase (Rand et al., 1993).

ΔH-ΔS compensation

Thus it is certain that the catalytic events in the active site are coupled with changes in the surface hydrophobicity of S1. This is probably the basis of thermodynamic characteristics of ATP cleavage and phosphate release steps in S1 ATP hydrolysis, where the enthalpy and entropy changes (ΔH and ΔS) have the same sign and proportionate magnitudes, so as to keep the standard Gibbs energy changes minimized: the Gibbs energy of S1·ATP, S1·ADP·P_i, and S1·ADP states are roughly on a level with each other (Kodama, 1985). Such ΔH-ΔS compensation effects are usually observed in related series of reactions of many proteins (e.g., binding of ligands of similar structures), which has long been a challenging issue in protein chemistry (Gregory, 1995). The entropy changes for the steps of S1·ATP hydrolysis can be ascribed to the S1 surface hydrophobicity changes as described above. In addition, on the basis of data tabulated by Tanford (1980), the enthalpy contribution to the hydrophobic interaction is very small if not totally negligible. Hence the large enthalpy changes observed in the steps of the ATPase cycle may be taken as the measure of the energy changes accompanying subtle structural changes involving the formation/breaking of hydrogen bonds and other weak interactions during the ATP hydrolysis reaction. If so, S1·ATP hydrolysis would be the first case in which the ΔH-ΔS compensation effect accompanying the steps of the catalytic cycle can be ascribed to the dynamic structural correlation of the active site with the molecular surface hydrophobicity. It is of great interest to examine whether the same applies to other protein reactions showing the ΔH-ΔS compensation effects.

As for a region or regions to which the hydrophobicity change is assigned, Gopal and Burke (1996) raised the possibility that a major hydrophobic crevice of S1 (Rayment et al., 1993) may be closed or tightened on ATP binding and hydrolysis, which would reduce the accessibility of the immobilized phenyl ligand into the crevice. However, the hydrophobic chromatography may also probe the hydrophobicity of the protein molecule as a whole, so that an involvement of other regions cannot be excluded. Thus the actin-binding interface is an equally plausible region, because the well-known ATP-induced decrease in the actin affinity of myosin can be mainly ascribed to a decrease in hydrophobicity of the interface. In the presence of ATP the affinity shows a stronger dependence on ionic strength (Chaussepied et al., 1988; Greene et al., 1983), indicating a diminished hydrophobic nature that is responsible for strong binding in the absence of nucleotide or in the presence of ADP alone. A recent van't Hoff analysis of temperature dependence of the affinity by Katoh and Morita (1996), in fact, indicates that a large decrease in the affinity (a lowered Gibbs energy decrease) in the presence of ATP is mostly due to a large decrease in entropy contribution.

It is pertinent to note here that among three different techniques used in recent studies of hydration or hydrophobicity changes of contractile proteins, the dielectric spectroscopy described here will have the least perturbation effect on the object of observation. Its major drawback is to require rather high protein concentrations, so that it is not practically applicable to actin-containing solutions by present instrumentation. The hydrophobic chromatography should be performed under high concentrations of ammonium sulfate (Gopal and Burke, 1996), which would affect the kinetics of ATP hydrolysis by S1 as well as by S1/actin system. For the osmotic stress method, the perturbation of the object itself is the very principle of measurement (Rand et al., 1993). However, it is the only one here that is applicable to experiments with actin-containing systems (Highsmith et al., 1996).

Taken together, it seems worth investigating further details of the protein surface hydrophobicity or the hydration changes observed in contractile proteins and their interactions from both experimental and theoretical viewpoints. When combined with atomic details of S1 structures with different bound nucleotides, this approach will lead to a major breakthrough in studying the mechanism of chemomechanical energy transduction.

We thank Dr. Tetsuya Tateishi for his support and Dr. Taro Q. P. Uyeda for many discussions. This work was supported by AIST and STA.

REFERENCES

Chaussepied, P., M. F. Morales, and R. Kassab. 1988. The myosin SH2-50-kilodalton fragment cross-link: location and consequences. *Biochemistry.* 27:1778–1785.

Eisenberg, D., and A. D. McLachlan. 1986. Solvation energy in protein folding and binding. *Nature.* 319:199–203.

Geeves, M. A., M. R. Webb, C. F. Midlefort, and D. R. Trentham. 1980. Mechanism of adenosine 5′-triphosphate cleavage by myosin: studies with oxygen-18-labeled adenosine 5′-triphosphate. *Biochemistry.* 21: 4748–4754.

Goldammer, E. v., and H. G. Hertz. 1970. Molecular motion and structure of aqueous mixtures with nonelectrolytes as studied by nuclear magnetic relaxation methods. *J. Phys. Chem.* 74:3734–3755.

Gopal, D., and M. Burke. 1996. Myosin subfragment 1 hydrophobicity changes associated with different nucleotide-induced conformations. *Biochemistry.* 35:506–512.

Grant, E. H., R. J. Sheppard, and G. P. South. 1978. Dielectric Behavior of Biological Molecules in Solution. Clarendon, Oxford.

Greene, L. E., J. Sellers, E., and A. S. Adelstein. 1983. Binding of gizzard smooth muscle myosin subfragment 1 to Actin in the presence and absence of adenosine 5′-triphosphate. *Biochemistry.* 22:530–535.

Gregory, R. B. 1995. Protein-Solvent Interactions. Marcel Dekker, New York.

Hanai, T. 1960. Theory of the dielectric dispersion due to the interfacial polarization and its application to emulsions. *Kolloid Z.* 171:23–31.

Highsmith, S., K. Duignan, R. Cooke, and J. Cohen. 1996. Osmotic pressure probe of actin-myosin hydration changes during ATP hydrolysis. *Biophys. J.* 70:2830–2837.

Katoh, T., and F. Morita. 1996. Binding of myosin subfragment 1 to actin. *J. Biochem.* 120:189–192.

Kodama, T. 1985. Thermodynamic analysis of muscle ATPase mechanisms. *Physiol. Rev.* 65:467–551.

Kodama, T., K. Fukui, and K. Kometani. 1986. The initial phosphate burst in ATP hydrolysis by myosin and subfragment-1 as studied by a modified malachite green method for determination of inorganic phosphate. *J. Biochem.* 99:1465–1472.

Levitt, M. 1992. Accurate modeling of protein conformation by automatic segment matching. *J. Mol. Biol.* 226:507–533.

Pethig, R., 1979. Dielectric and Electronic Properties of Biological Materials. Wiley, New York.

Rand, R. P., N. L. Fuller, P. Butko, G. Francis, and P. Nicolls. 1993. Measured change in protein solvation with substrate binding and turnover. *Biochemistry.* 32:5925–5929.

Rayment, I., W. R. Rypniewski, K. Schmidt-Base, R. Smith, D. R. Tomchick, M. M. Benning, D. A. Winkelmann, G. Wesenberg, and H. M. Holden. 1993. Three-dimensional structure of myosin subfragment-1: a molecular motor. *Science.* 261:50–58.

Rossky, P. J., and M. Karplus. 1979. Solvation. A molecular dynamics study of a dipeptide in water. *J. Am. Chem. Soc.* 101:1913–1937.

Ruppel, K. M., and J. A. Spudich. 1996. Structure-function studies of the myosin motor domain: importance of the 50-kDa cleft. *Mol. Biol. Cell.* 7:1123–1136.

Suzuki, M., J. Shigematsu, and T. Kodama. 1996. Hydration study of proteins in solution by microwave dielectric analysis. *J. Phys. Chem.* 100:7279–7282.

Takashima, S. 1989. Electrical Properties of Biopolymers and Membranes. Adam Hilger, Philadelphia.

Tamura, Y., N. Suzuki, and K. Mihashi. 1993. Adiabatic compressibility of myosin subfragment-1 and heavy meromyosin with or without nucleotide. *Biophys. J.* 65:1899–1905.

Tanford, C. 1980. The Hydrophobic Effect. Wiley, New York.

Wagner, K. W. 1914. Erklarung der dielektrischen nachwirkungsvorgange auf grund Maxwellscher vorstellungen. *Arch. Electrotech.* 2:371–387.

Weeds, A. G., and R. S. Taylor. 1975. Separation of subfragment-1 isoenzymes from rabbit skeletal muscle myosin. *Nature.* 257:54–56.

Wei, Y. Z., A. C. Kumbharkhane, M. Sadeghi, J. T. Sage, W. D. Tian, P. M. Champion, S. Sridhar, and M. J. McDonald. 1994. Protein hydration investigations with high-frequency dielectric spectroscopy. *J. Phys. Chem.* 98:6644–6651.

Woledge, R. C., N. A. Curtin, and E. Homsher. 1985. Energetic Aspects of Muscle Contraction. Academic Press, London.